MAGNETOHYDRODYNAMICS Vol. 58 (2022), No. 4, pp. 435–443
DOI: 10.22364/mhd.58.4.7

NONLINEAR LAMINAR 'DYNAMOS' LINEAR IN ONE COORDINATE

A.J. Mestel, A. Arslan, R.H. Vaz, E. Mancini

Mathematics Department, Imperial College London SW7 2BZ, UK

We consider two self-similar flow fields, for which the Navier–Stokes equations reduce to ODEs. If the magnetic field has a similar structure, then the induction equation also reduces to ODEs. The coupled system can be regarded as a kinematic dynamo problem, but also the fields grow until they saturate as exact solutions of the nonlinear system. The extent to which these solutions can be regarded as genuine dynamos is discussed.

Introduction.

Exact solutions of the kinematic dynamo problem are rare, and almost none of these can be followed into the nonlinear regime. In this paper we investigate two flow structures which do permit this. The first resembles axisymmetric stagnation flow between two cylinders near a reversal in the direction of swirl. The other is von-Kármán flow between two differentially rotating infinite discs. Each of our chosen flows is linear in one coordinate. This implies that both the Laplacian and the Jacobians are also linear in that coordinate, which, therefore, cancels from the problem. This simplification reduces the Navier–Stokes equations to a pair of ODEs. Magnetic fields are sought with a similar spatial structure and so the induction equation also reduces to ODEs. Both the kinematic dynamo problem and the fully nonlinear system can, therefore, be solved fairly easily. The flows and fields we consider are axisymmetric, but as the domain is unbounded, the system does not run foul of Cowling's anti-dynamo theorem [1].

The fact that our solutions involve motion and magnetic field at infinity makes it important to consider whether they are being driven by local considerations or whether energy is being advected in from infinity. Some growing fields are found to be fed from the distant boundary conditions, but others are not, and we refer to solutions for which the net flux of magnetic energy is outwards as dynamos. We argue that these may be the local form of genuine dynamos in a finite container, such as the VKS experiments [2, 3].

We consider a laminar, incompressible velocity field $\mathbf{u}$ and a magnetic field $\mathbf{B}$ with associated vorticity $\boldsymbol{\omega}$ and current density $\mathbf{j}$ satisfying the induction equation

$$\lambda\mathbf{B} = \mathrm{rot}(\mathbf{u}\times\mathbf{B}) + \mathrm{Rm}^{-1}\nabla^2\mathbf{B}, \tag{1}$$

and the curl of the steady Navier–Stokes equation

$$0 = \mathrm{rot}(\mathbf{u}\times\boldsymbol{\omega}) + \mathrm{rot}(\mathbf{j}\times\mathbf{B}) + \mathrm{Re}^{-1}\nabla^2\boldsymbol{\omega} \tag{2}$$

together with the solenoidal conditions

$$\mathrm{div}\,\mathbf{u} = 0 = \mathrm{div}\,\mathbf{B}. \tag{3}$$

The Reynolds number and magnetic Reynolds numbers are denoted by Re and Rm, respectively. In Eq. (1), λ is the growth rate of the field in the kinematic dynamo problem. For the coupled steady solutions, we set $\lambda = 0$. The similarity between the governing equations is clear, and so it is natural to seek solutions to the coupled problem

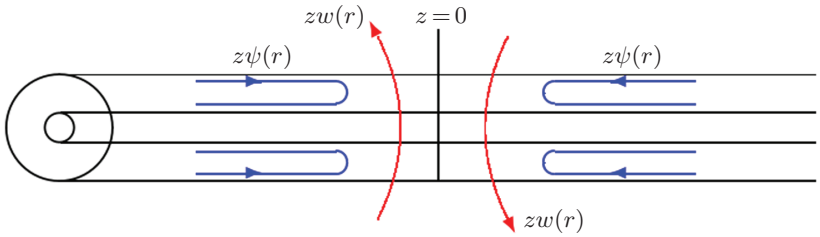

Fig. 1. Schematic of twist reversal flow. The azimuthal velocity $zw(r)$ changes direction at $z=0$ inducing a poloidal flow given by the streamfuction $z\psi(r)$.

with a similar spatial dependence. For example, we could find axisymmetric solutions to Eq. (2) with $\mathbf{B}=0$ and, if that drives a kinematic dynamo, we could then seek consistent axisymmetric fields $\mathbf{u}$ and $\mathbf{B}$ to the coupled system. In a finite container, we know such an enterprise is doomed by Cowling's theorem [1], but in an unbounded domain, saturated solutions can exist.

Further examples are the helically symmetric flows considered by Zabielski & Mestel [4, 5], which give rise to coupled helically symmetric fields. For that problem, the field can saturate at a steady value, be time-periodic, nearly periodic or chaotic. The solutions may also exhibit polarity reversals and intermittent quenching [5].

In this paper we shall consider two simple axisymmetric flows, each linear in a coordinate. This has the advantage that the Laplacians are also linear in that coordinate, as are the Jacobians implicit in the nonlinear terms such as $\mathbf{u}\cdot\nabla\mathbf{B}$. As a result, this coordinate may disappear from the problem. This can have the effect of reducing two-dimensional PDES to a system of ODEs, greatly simplifying the problem. We use cylindrical polar coordinates $(r,\,\theta,\,z)$. In Section 1 we consider flows and fields essentially linear in z, while in Section 2 we consider von Kármán flows linear in r. In Section 3 we investigate the direction of the magnetic energy flux for these solutions. We conclude in Section 4.

1. Twist reversal in an annulus.

We consider the region between two cylinders, $a<r<b$, and seek velocities of the form

$$\mathbf{u}=\left(\frac{-\psi(r)}{r},\, zw(r),\, \frac{z\psi'}{r}\right), \tag{4}$$

where $\psi(r)$ and $w(r)$ are to be found subject to the solid boundary conditions

$$\psi=\psi'=w=0 \qquad \text{on} \quad r=a,\,b.$$

This flow can be regarded as the local behaviour of an azimuthal swirl changing sign at $z=0$, as depicted in Fig. 1. Substituting in Eq. (2) gives rise to the equations

$$\begin{aligned}
\psi' w-\psi w'-\frac{w\psi}{r}&=\mathrm{Re}^{-1}\left[rw''+w'-\frac{w}{r}\right],\\
\psi'\psi''-\psi\psi'''+\frac{3\psi\psi''}{r}-\frac{\psi'^2}{r}-\frac{3\psi\psi'}{r^2}+2rw^2&=\mathrm{Re}^{-1}\left[r\psi''''-2\psi'''+\frac{3\psi''}{r}-\frac{3\psi'}{r^2}\right].
\end{aligned} \tag{5}$$

These equations and boundary conditions have no explicit forcing. Nevertheless, it was shown in [6] that they possess more than one solution, with the velocity $\mathbf{u}\propto\mathrm{Re}^{-1}$.

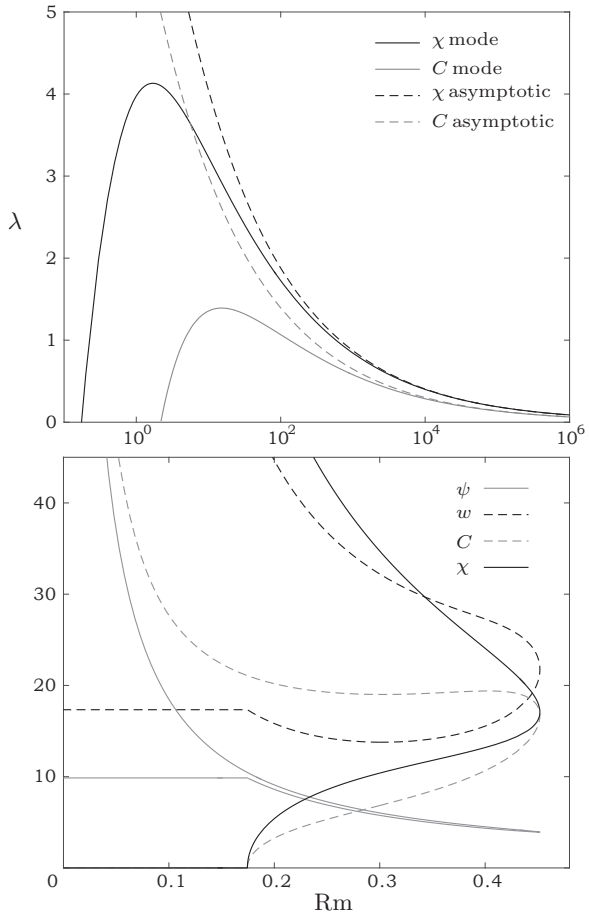

Fig. 2. Top: Growth rate $\lambda(\mathrm{Rm})$ for $1 < r < 3$ with asymptotic behaviour for large Rm. Bottom: Norms of the nonlinear saturated solution, showing hysteresis and sub-critical solutions.

These flows are essentially forced from infinity. We choose one such flow and seek a kinematically growing field of similar form,

$$\mathbf{B} = \left(-\frac{\chi(r)}{r},\, zC(r),\, z\frac{\chi'(r)}{r} \right) \mathrm{e}^{\lambda t}. \tag{6}$$

Either perfectly conducting or insulating boundary conditions are imposed on $r = a, b$. In each case, growing modes are found for fairly low values of the magnetic Reynolds number Rm. The growth rate of the kinematic eigenfunction as Rm varies for two different modes is drawn at the top of Fig. 2. Also shown is the asymptotic behaviour of λ for large Rm, which is determined by the boundary layer on the outer cylinder, $r = b$, as shown in [7].

As the field grows, it reacts back on the driving flow, and the system saturates in steady states which can be found by substituting Eqs. (4) and (6) into Eqs. (1) and (2) with $\lambda = 0$. This leads to 4 simultaneous ODEs in ψ, w, C and χ. Once one solution has been found, path continuation techniques [8, 9] are used to follow the solution branches as Rm varies. The solution behaviour is illustrated at the bottom of Fig. 2. The solution

branches link to the critical Rm values for dynamo action, but subcritical solutions exist for larger field values. The system exhibits hysteresis, with the low amplitude solution disappearing as Rm increases. Note that because $\mathbf{u} \sim \mathrm{Re}^{-1}$ for this flow, one should really think of Rm as a magnetic Prandtl number.

2. Von Kármán flow between two discs.

The second flow we consider is the von Kármán flow between two differentially rotating discs, for which

$$\mathbf{u} = (-rH'(z),\, rG(z),\, 2H(z)) \qquad \text{in } 0 < z < 1. \tag{7}$$

The Navier–Stokes equations with $\mathbf{B} = 0$ take the form

$$G" = 2\mathrm{Re}(HG' - GH'), \qquad H'''' = 2\mathrm{Re}(HH''' + GG') \tag{8}$$

with

$$H(0) = H'(0) = H(1) = H'(1) = 0, \qquad G(0) = 1, G(1) = s. \tag{9}$$

The flow has been non-dimensionalised with respect to the rotation of the lower disc. When $s = 1$, the flow is solid body rotation, but when $s \neq 1$, there are several hydrodynamic solution branches for fixed Re and s, as investigated in [10–12]. The various solutions differ mainly in their poloidal velocity structure, as shown at the top of Fig. 3. At the bottom of this figure the Batchelor branch (blue) is sketched, where the main body of the flow is almost in solid body rotation and the flow is directed towards the lower disc.

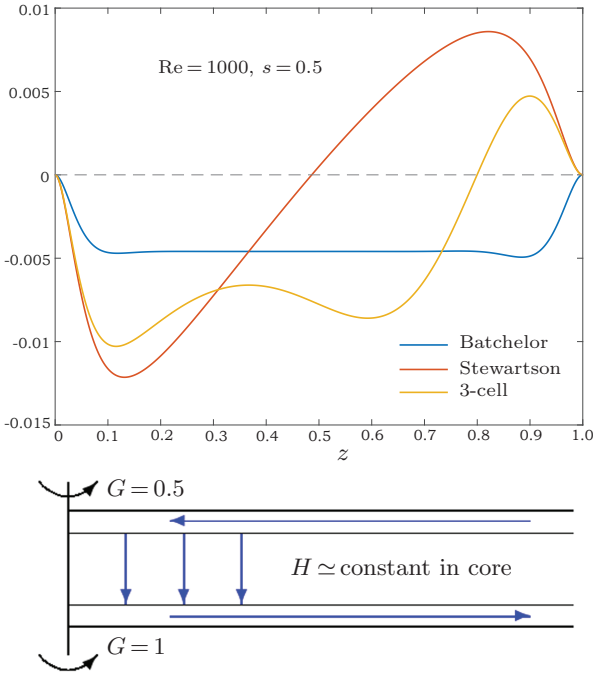

Fig. 3. Top: $H(z)$ for 3 solutions for von Kármán flow when $s = 0.5$ and $\mathrm{Re} = 1000$. bottom: Schematic of flow for the Batchelor branch for which $H < 0$.

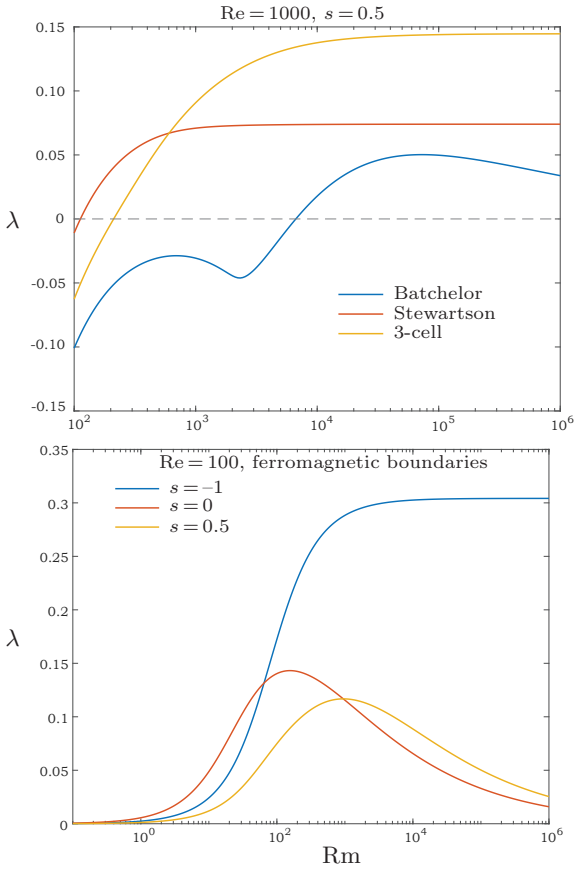

Fig. 4. Growth rate as a function of Rm. Top: three branches for conducting discs, Re = 1000, $s = 0.5$. The Stewartson branch is fast. Bottom: Stewartson branch for perfectly ferromagnetic discs, Re = 100 and different s. The case $s = -1$ is fast.

In contrast, for the Stewartson branch (red) the flow is directed towards both discs.

We once more seek a co-existing magnetic field with a similar spatial structure, namely,

$$\mathbf{B} = (-rP'(z),\, rT(z),\, 2P(z))\, e^{\lambda t}. \tag{10}$$

The induction equation becomes

$$\lambda T + 2HT' - 2G'P = \mathrm{Rm}^{-1} T'', \tag{11}$$

$$\lambda P + 2HP' - 2H'P = \mathrm{Rm}^{-1} P'' \tag{12}$$

We see that, as usual, the toroidal field does not appear in the poloidal equation. For the nonlinear steady states we again set $\lambda = 0$ and we obtain 4 coupled ODEs for G, H, T and P. We consider 3 types of boundary conditions on the rotors at $z = 0, 1$: insulating, perfectly conducting and perfectly ferromagnetic. Kinematic growth is found in all cases, but the ferromagnetic boundary condition is found to be particularly favourable. This agrees in broad terms with the results of the Von-Kármán-Sodium experiment [2, 3] which found dynamo action when the rotors were constructed from iron with a high permeability.

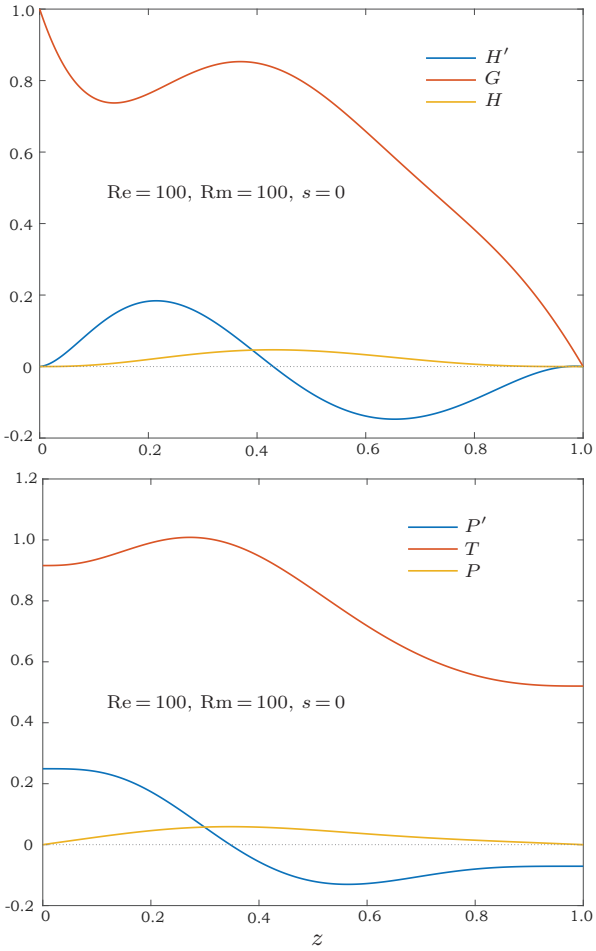

Fig. 5. Equilibrium for $\mathrm{Re} = 100 = \mathrm{Rm}$ and $s = 0$. Top: flow, bottom: field.

As shown in [13], an interesting feature is that for some flow fields, the 'dynamo' can be 'fast', meaning that $\Re\mathrm{e}\,(\lambda) \to \lambda_\infty > 0$ as $\mathrm{Rm} \to \infty$. This is illustrated in Fig. 4, which shows the growth rate for various flows and parameters.

Only flows for which the poloidal flow is directed towards each disc are 'fast', as discussed in the next section. The unstable modes can be followed into the nonlinear regime. For example, the saturated equilibrium resulting from an initially Stewartson branch for $\mathrm{Re} = \mathrm{Rm} = 100$ and $s = 0$ is shown in Fig. 5.

3. Where does the magnetic energy come from?

We have found growing fields in various ranges of the parameters $(\mathrm{Re}, s, \mathrm{Rm})$. However, the domain is unbounded and both the kinetic and the magnetic energy densities scale with r^2 as $r \to \infty$. In reality, our solutions must be regarded as a local representation near $r = 0$ of global fields. Even if there is a process for local field generation, it is certainly possible that conditions at large r will destroy this growth. But also, there is the possibility that the field is not actually being generated near $r = 0$, but is instead being advected in from large r. Similar comments apply also to the flow we considered in Section 1. In that case, there was no local generation of the flow, so certainly the

velocity was being driven at large $|z|$.

We can examine the energy fluxes of our solutions. Taking the scalar product of the induction equation (1) with $\mathbf{B}$ and integrating over the volume $0 < z < 1$, $0 < r < R$, we obtain

$$\frac{\mathrm{d}}{\mathrm{d}t}\int \frac{1}{2}\mathbf{B}^2\,\mathrm{d}V = -\int \mathbf{u}\cdot\mathbf{j}\times\mathbf{B}\,\mathrm{d}V - \mathrm{Rm}^{-1}\int \mathbf{j}^2\,\mathrm{d}V - \oint_{r=R} \mathbf{E}\times\mathbf{B}\cdot\mathbf{n}\,\mathrm{d}S, \qquad (13)$$

where we have introduced the electric field $\mathbf{E} = \mathrm{Rm}^{-1}\mathbf{j} - \mathbf{u}\times\mathbf{B}$ and $\mathbf{n}$ denotes the normal in the r-direction. The first three terms in Eq. (13) are readily understood as the rate of change of magnetic energy, the rate at which the fluid does work on the magnetic field and Joule dissipation. The last term, which we call M, indicates the rate at which energy is transported across the boundary at large r by the Poynting vector $\mathbf{E}\times\mathbf{B}$. For each of our solutions we can evaluate M, the magnetic energy flux across $r = R$. If this flux is inwards, then the field growth is driven from infinity, but if it is outwards, then we can regard the flow as a local dynamo. We can do this both for the kinematic growing modes and for the saturated states.

As one might expect, we find that all the fast dynamo modes of Stewartson [11] type involve an influx of energy from infinity, as in Fig. 6 (top). However, many of the Batchelor [10] branches do give rise to an outwards energy flux, as in Fig. 6 (middle). These branches involve a z-component of velocity away from one disc and towards the other. In the limit of high Rm it can be shown that the growth rate λ is determined by

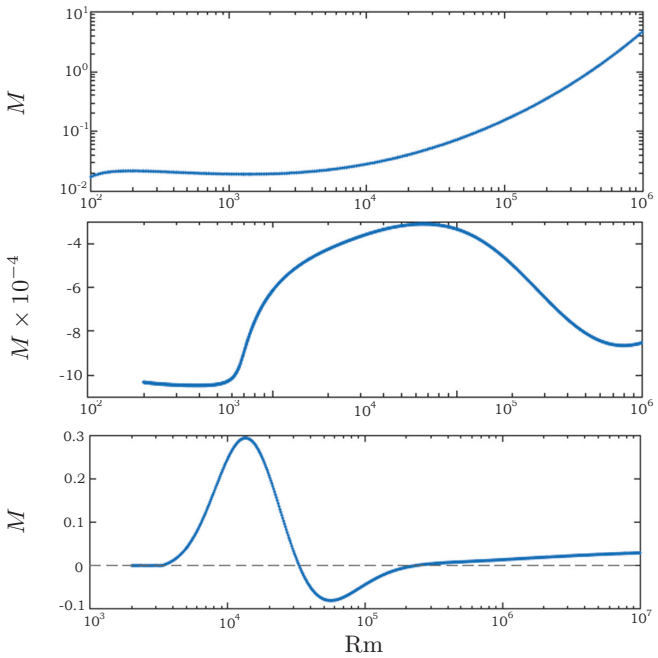

Fig. 6. Magnetic energy flux. Top: $M > 0$ inward, $\mathrm{Re} = 500$, $s = -1$, Stewartson branch. Middle: $M < 0$ outward, $\mathrm{Re} = 1000$, $s = 0.8$, steady equilibrium with insulating walls. Bottom: the sign of flux varies with Rm, $\mathrm{Re} = 500$, $s = 0.5$, Batchelor branch, both kinematic with perfectly conducting walls.

a boundary layer on the former disc of thickness of the order $(\mathrm{Rm})^{-1/3}$, confirming the 'slow' nature of the dynamo (compare Fig. 2). Occasionally, we found that the magnetic energy flux M can be either inward or outward depending on the value of Rm, as in Fig. 6 (bottom).

4. Concluding remarks.

We have demonstrated the existence of local solutions to both the Navier–Stokes and the magnetic induction equations with simple spatial structures. These solutions may generate magnetic energy locally and could arguably constitute the engine in a global dynamo in a finite container. At the very least, they provide the local form of hydromagnetic equilibria for more general problems. However, the unbounded flows we have considered are axisymmetric, and even if they generate magnetic energy locally, the constraints of Cowling's theorem [1] would require non-axisymmetric closure in a finite container for a genuine dynamo.

It should not be forgotten that even when there is a growing mode with a structure similar to the velocity, this may not be the most unstable kinematic mode. Thus, for an unbounded axisymmetric velocity we have also investigated the growth of non-axisymmetric fields proportional to $\exp(im\theta)$. For the von Kármán flow over a single disc, the ansatz (10) can be replaced by

$$\mathbf{B} = \big(rQ(z),\, rT(z),\, R(z)\big)\mathrm{e}^{im\theta}\mathrm{e}^{\lambda t}, \tag{14}$$

but this representation is no longer exact because the angular term introduces different powers of r into the Laplacian. However, in the high-Rm limit, the diffusive terms are only significant in layers near the boundary, where $\mathrm{d}^2/\mathrm{d}z^2 \gg m^2/r^2$. As a result, in this limit the system reduces to ODEs similar to Eq. (11) with a similar asymptotic behaviour. The value of this approach is limited, however, as when the nonlinear problem is considered, the simple structure is destroyed as more azimuthal modes are excited by the quadratic interactions.

Finally, it must be remembered that the assumption of laminar flow is critical in permitting fully non-linear solutions to be found. The low magnetic Prandtl number of liquid metals ensures turbulent flow in the laboratory and some of the detailed features of these solutions may not be realised in practice.

Acknowledgements.

The authors are grateful for the support of EPSRC and the CDT for Fluid Dynamics across Scales at Imperial College London.

References

[1] T.G. Cowling. The magnetic field of sunspots. *MNRAS*, vol. 94 (1933), no. 1, pp. 39–48.

[2] C. Nore, D. Castanon Quiroz, L. Cappanera, and J.-L. Guermond. Numerical simulation of the von Kármán sodium dynamo experiment. *J. Fluid Mech.*, vol. 854 (2018), pp. 164–195.

[3] M. Berhanu *et al.* Dynamo regimes and transitions in the VKS experiment. *Eur. Phys. J. B*, vol. 77 (2010), pp. 459–468.

[4] L. Zabielski and A.J. Mestel. A double helix laminar dynamo. *J. Fluid Mech.*, vol. 573 (2007), pp. 237–246.

[5] L. Zabielski and A.J. Mestel. Nonlinear dynamos in laminar, helical pipe flow. *Physics of Fluids*, vol. 18 (2006), p. 043602.

[6] R.H. Vaz, F.A.T. Boshier, and A.J. Mestel. 'unforced' navier–stokes solutions derived from convection in a curved channel. *J. Fluid Mech.*, vol. 848 (2018), pp. 676–695.

[7] R.H. Vaz, F.A.T. Boshier, and A.J. Mestel. Dynamos in an annulus with fields linear in the axial coordinate. *Geophys. Astrophys. Fluid Dyn.*, vol. 112 (2018), pp. 222–234.

[8] E.L. Allgower and K. Georg. Continuation and path following. *Acta Numerica*, vol. 2 (1993), pp. 1–64.

[9] T.F. Chan. Newton-like pseudo-arclength methods for computing simple turning points. *SIAM J. Sci. and Stat. Comput.*, vol. 5 (1984), no. 1, pp. 135–148.

[10] G. Batchelor. Note on a class of solutions of the navier–stokes equations representing steady rotationally-symmetric flow. *Quart. J. Mech. Appl. Math*, vol. 4 (1951), pp. 29–41.

[11] K. Stewartson. On the flow between two rotating coaxial discs. *Math. Proc. Cam. Phil. Soc.*, vol. 49 (1953), pp. 333–341.

[12] P.J. Zandbergen and D. Dijkstra. Von kármán swirling flows. *Ann. Rev. Fluid Mech.*, vol. 19 (1987), pp. 465–91.

[13] A. Arslan and A.J. Mestel. Dynamo action between two rotating discs. *Geophys. Astrophys. Fluid Dyn.*, vol. 115 (2021), pp. 710–727.

Received 07.10.2022